Amplitude-modulated electrostatic nanolithography in polymers based on atomic force microscopy

Sergei F. Lyuksyutov[a] and Pavel B. Paramonov
Department of Physics, The University of Akron, Akron, Ohio 44325

Shane Juhl and Richard A. Vaia
Materials and Manufacturing Directorate, Air Force Research Laboratory, Wright-Patterson Air Force Base, Ohio 45433

(Received 9 July 2003; accepted 29 September 2003)

Amplitude modulated electrostatic lithography using atomic force microscopy (AFM) on 20–50 nm thin polymer films is discussed. Electric bias of AFM tip increases the distance over which the surface influences the oscillation amplitude of an AFM cantilever, providing a process window to control tip-film separation. Arrays of nanodots, as small as 10–50 nm wide by 1–10 nm high are created via a localized Joule heating of a small fraction of polymer above the glass transition temperature, followed by electrostatic attraction of the polarized viscoelastic polymer melt toward the AFM tip in the strong (10^8-10^9 V/m) nonuniform electric field. © *2003 American Institute of Physics.* [DOI: 10.1063/1.1629787]

Scanning probe microscopy (SPM)-based lithographic techniques have proven to be extremely flexible patterning tools, enabling atomic assembly,[1] chemical (''dip-pen'') patterning,[2] and topological sculpturing.[3] The ubiquitous presence of polymers in high technology processes, devices, and products drives innovations specific for nanolithographic patterning of polymers. Earlier SPM techniques such as thermal-mechanical writing[4] and latent image formation[5] established the atomic force microscopy (AFM) cantilever as a valuable tool for nanoscale patterning of thin polymer films. Recent advances in multicantilever arrays have catapulted these techniques from slow serial procedures to industrial prototypes, such as exemplified with MILLIPEDE[6,7] (based on thermal-mechanical lithography) and[2] (based on dip-pen nanolithography).

Recently, Lyuksyutov and co-workers reported a SPM patterning approach that is based on localized Joule heating and dielectrophoritic manipulation of a thin polymer film and is compatible with multicantilever array technology.[8] Current flow through a thin polymer film, arising from a bias between a conductive substrate and AFM tip, results in localized Joule heating of attoliters of polymer above its glass transition temperature. Polarization and electrostatic attraction of the molten polymer toward the AFM tip in the strong (10^8-10^9 V/m) nonuniform electric field is believed to produce raised structures. Initial studies using AFM-based electrostatic nanolithography (AFMEN) demonstrated feature formation in a broad range of polymers with different physical-chemical properties. The rate of feature formation was estimated to be on the order of microseconds and final feature size depended on the magnitude of current through the polymer film. Electronic breakdown of the polymer was critical for the onset of current flow, heat flow into the polymer film, and the amount of softened dielectric polymer and thus feature size.

Control of the dielectric breakdown and elucidation of its relationship to feature size is the critical controllability issue for AFMEN. The major factors affecting dielectric breakdown are suspected to be (i) AFM tip-polymer film separation; (ii) thickness of the polymer film; and (iii) mechanism of conductivity, apparently associated with negative carriers either migrating from the Fermi level of the tungsten-carbide coated AFM tip, or generated through the electric breakdown in water attracted to an AFM tip.[9]

To begin to address these issues, the influence of tip-film separation though the use of amplitude-modulated (tapping) AFM is examined herein. In contrast to contact mode, amplitude-modulated (AM) mode provides more flexibility in controlling configuration of the tip-surface junction, tip motion, and its interaction with the sample, allowing a wider range of writing conditions and producing smaller nanostructures with larger aspect ratios.

A schematic presentation of the AM–AFMEN process is shown in Fig. 1. A conductive AFM tip is driven by a piezoelement to oscillate above the film at 200–400 kHz. Figure 2(a) presents typical amplitude-distance relationships for tip oscillating without negative bias (curve 1) and with negative bias (curves 2 and 3) where the feedback loop was disabled (i.e., piezoelement does not compensate for surface-induced damping of the oscillation amplitude). The oscillation amplitude of an unbiased cantilever depends on the piezoscanner drive voltage and frequency, as well as the mechanical and geometrical characteristics of the cantilever. At a critical distance, van der Waals and coulombic forces overcome the driving force of the piezoscanner, rapidly decreasing the oscillation amplitude to zero (steep portion of curve 1). When the amplitude goes to zero, the tip is in contact with surface. With an applied dc bias between the tip and substrate, the influence of coulombic force extends the tip-surface interaction distance, impacting cantilever oscillation at greater distances (curves 2 and 3). The extent of these additional interactions is proportional to the magnitude of the bias voltage (-10 to -50 V).

[a]Electronic mail: sfl@physics.uakron.edu

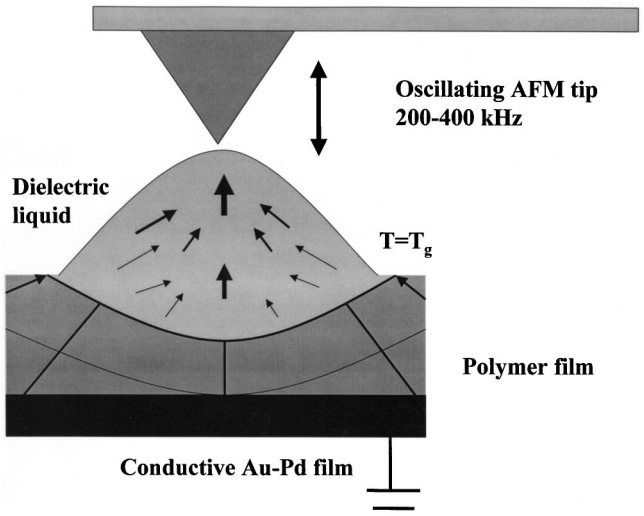

FIG. 1. Schematic presentation of AM–AFMEN experimental setup. An AFM tip oscillates 0–300 nm above polymer film at 200–400 kHz.

The extended range and oscillating character of tip-surface interactions improves process control. Previous time-dependent heat transfer calculations indicated that a stable, sustained temperature rise above the glass transition temperature (T_g) for a small fraction of the polymer under the AFM tip can be established in microseconds.[10] For 200–400 kHz oscillation, tip-surface contact is also in the microsecond range, implying each tap is a discrete event. The pulsating character of the tip-surface interaction should provide enhanced control over current injection and electronic breakdown of the film. Additionally, altering the cantilever oscillation frequency refines the ability to control heat generation, and subsequent material deformation. Finally, noncontact or related AFM modes (as tapping) are easily adapted to multiple AFM tip arrays due to minimization of lateral forces and short contact time.[11,12]

Typical structures lithographically patterned into polymethylmethacrylate (PMMA) (MW$\sim$980 000) and polystyrene (PS) (MW$\sim$2350, 110 000, 2 800 000) films are presented in Fig. 3. A thin polymer layer [20–50 nm; roughness nominally less than 0.2 nm (tapping AFM imaging)] is spun cast onto a conductive Au–Pd film evaporated onto silicon. A small portion of the polymer film is removed to attach an electrode to the Au–Pd layer. Features are created using a Digital Instruments 3100 Dimensions AFM in amplitude modulated taping mode with a range of bias voltages between -5 and -50 V. Amplitude near the resonant frequency (200–400 kHz) of the cantilever of the highly conductive W_2C covered AFM tips was 10–50 nm. The spring constant of the tips was between 3 and 30 N/m. Electric current was in the range from 10^{-11} to 10^{-8} A and monitored with a Keithley 6485 picoammeter. With the feedback loop disbled, the tip is initially brought toward the polymer surface until the oscillation amplitude decreases to zero. This tip position is used as the initial reference point, setting the tip-film separation, $d=0$. The tip is then retracted, translated into position and tip-film separation is adjusted to the desired oscillation amplitude with the feedback loop enabled. Finally feedback loop disabled again and dc voltage pulse, significantly exceeding the oscillation period (typically by the factors of 10^1-10^5) is applied. Note that feature formation occurs with an oscillating tip-surface distance. Re-engaging the feedback loop and returning the amplitude to a conventional imaging value (80%–90% of free amplitude), topography of the created feature is obtained. Note that although the discussion is focused on dc-biased AM–AFMEN, preliminary data indicate that feature formation also occurs for ac voltage modulated AFMEN.

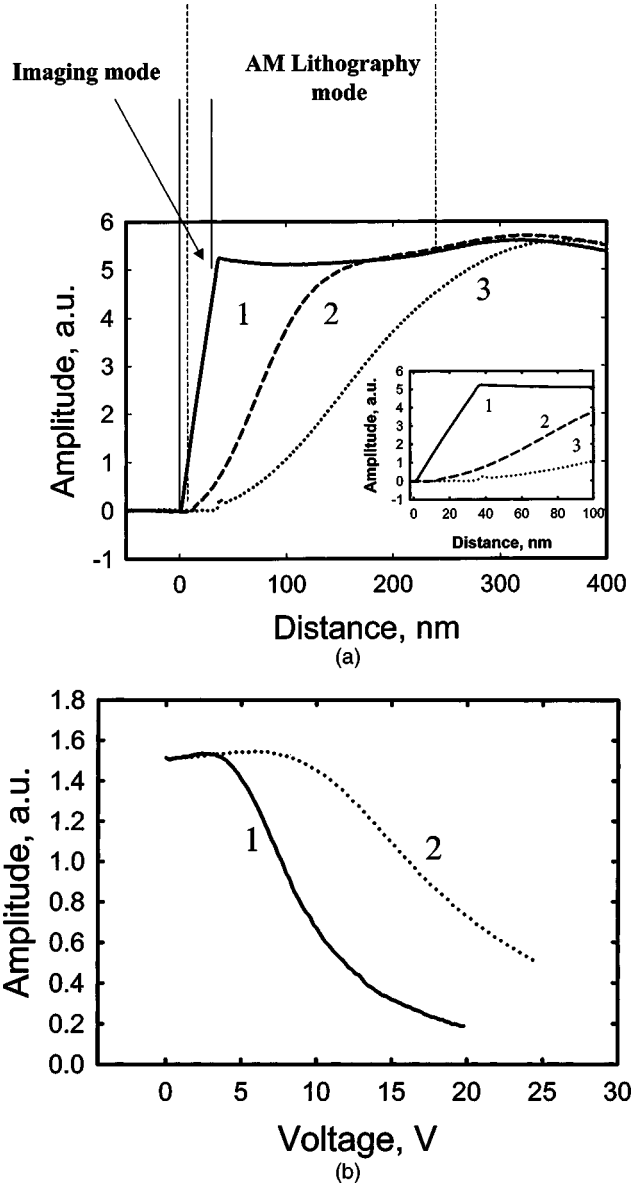

FIG. 2. (a) Dependence of the oscillating amplitude of the tip with respect to tip-film separation without (curve 1: 0 V), and with bias voltages (curve 2: -9 V, curve 3: -18 V) for 35 nm PS film span on Au–Pd substrate. The piezoelement feedback loop was disabled. $d=0$ corresponds to physical contact between the tip and surface. Tip maintains surface contact until a critical distance where oscillation amplitude increases with increasing separation. Inset: Expanded region of amplitude-distance dependence when the tip is near the surface. (b) For the same sample dependence of the oscillation amplitude on bias voltage for two different tip-film distances: 30 nm (curve 1) and 50 nm (curve 2).

Assuming the raised features are formed by mass-transport, the polymer should not be degraded. Therefore, the raised nanostructures are erasable by simple annealing of the film above the polymer's glass transition temperature and allowing surface tension to minimize surface area. Figure 3(e) presents AM–AFMEN-written nanodots on the surface

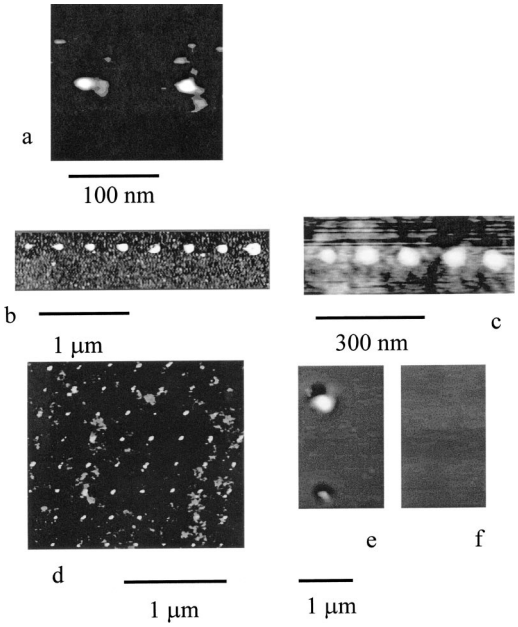

FIG. 3. Examples of patterned nanodots: (a) A fragment of a nanodot array: two nanodots 21 nm wide and 1 nm high in 20-nm-thick PS film (bias voltage -10 V, exposure -1 s). (b) A row on nanodots 60–80 nm wide and 8–15 nm high in 25-nm-thick PMMA film (bias voltage increasing from 25 V at 0.1 V per dot, exposure time -5 s). (c) A row of nanodots 30–50 nm wide and 1.5–4.5 nm high in 20-nm-thick PMMA film (bias voltage increasing from 29 V at 0.1 V per dot, exposure time is 1 s). (d) 8×8 array of nanodots in 25-nm-thick PS film (bias voltage begins at -32 V and ends at -38.4 V, exposure time 1 s per dot). (e) A portion of dot array made in 30 nm PS film [bias voltage -24 V (top), -16 V (bottom), exposure time is 3 s]. (f) Same spot after annealing the film at 130 °C for 20 min. PMMA and PS films were spun coated at 2500–3000 rpm and 6000 rpm, each for 20 s, on Au–Pd evaporated onto silicon substrate, then baked at 80 °C for 10 min in vacuum. The concentration of PMMA and PS was 0.5% wt and 1.03% in toluene, respectively.

of the PS film of 30 nm thick under ambient humidity. The dots are completely removed (f) after annealing the sample at $T=130$ °C in a vacuum chamber for 20 min.

The dependence on bias voltage of feature aspect ratio of patterned nanodots in PS film is shown in Fig. 4. The aspect (height-to-width) ratio of the nanostructures is as large as 0.1–0.2. This is substantially greater than that previously reported for AFMEN using contact mode,[8] or in scanning probe oxidation.[3] The shape (mostly asymmetric) of the AM–AFMEN-patterned dots depends on the magnitude and spatial distribution of the electric field near the tip. Voltage–current behavior during data collection was linear and corresponds to current dependent feature formation reported in Ref. 8. The pulsating tip-surface distance is suspected to mediate catastrophic dielectric breakdown of the film.

In summary, amplitude-modulated AFM-assisted electrostatic nanolithography is demonstrated as a technique for robust nanopattering of dots in 20–50-nm-thick films of PMMA and polystyrene. The width of the dots varies from

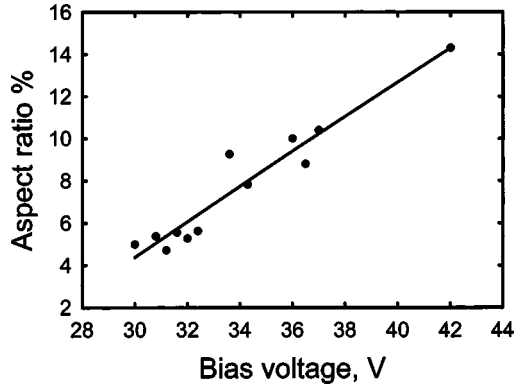

FIG. 4. Aspect ratio dependence on the bias voltage for 35 nm PS film on conductive Au–Pd substrate.

10 to 50 nm depending on tip-film separation and bias voltage. The aspect ratio achieved through AM–AFMEN was found to be 20%. This technique is a paradigm for nanolithography in which polymer features are generated by mass transport within a planar film in a single-step process and without external heating or direct contact. In this way, surface patterning can be achieved with high resolution and potentially much higher processing speed than with existing methods.

S.F.L. acknowledges support from National Research Council under Summer 2003 Faculty Research Fellowship program, AFOSR Grant No. F49620-02-1-0428, and Materials and Manufacturing Directorate of Air Force Research Laboratory at Wright-Patterson Air Force base for hospitality.

[1] H. Manoharan, C. P. Lutz, and D. M. Eigler, Nature (London) **403**, 512 (2000).
[2] R. D. Piner, J. Zhu, F. Xu, F. Hong, and C. Mirkin, Science **283**, 661 (1999).
[3] *Procedures in Scanning Probe Microscopies*, edited by R. J. Colton, A. Engel, J. E. Frommer *et al.* (Wiley, Chichester, 1999).
[4] H. J. Mamin and D. Rugar, Appl. Phys. Lett. **61**, 1003 (1992).
[5] A. Majumdar, P. I. Oden, J. P. Carrejo, L. N. Nagahara, J. J. Graham, and J. Alexander, Appl. Phys. Lett. **61**, 2293 (1992).
[6] P. Vettiger, M. Despont, U. Drechsler, U. Durig, W. Haberle, M. I. Lutwyche, H. E. Rothuizen, R. Stutz, R. Widmer, and G. K. Binning, IBM J. Res. Dev. **44**, 323 (2000).
[7] P. Vettiger, G. Cross, M. Despont, D. Drechsler, U. Durig, B. Gotsmann, W. Haberle, M. A. Lantz, H. E. Rothuizen, R. Stutz, and G. K. Binning, IEEE Trans. Nanotech. **1**, 39 (2002).
[8] S. F. Lyuksyutov, R. A. Vaia, P. B. Paramonov, S. Juhl, L. Waterhouse, R. M. Ralich, G. Sigalov, and E. Sancaktar, Nat. Mater. **2**, 468 (2003).
[9] S. F. Lyuksyutov, P. B. Paramonov, I. Dolog, and R. M. Ralich, Nanotechnology **14**, 716 (2003).
[10] The calculations of thermal equilibrium time is presented in supporting material online in S. F. Lyuksyutov, R. A. Vaia, P. B. Paramonov, S. Juhl, L. Waterhouse, R. M. Ralich, G. Sigalov, and E. Sancaktar, Nat. Mater. **2**, 468 (2003).
[11] K. Wilder, C. F. Quate, D. Adderton, R. Bernstein, and V. Elings, Appl. Phys. Lett. **73**, 2527 (1998).
[12] R. Garcia, M. Calleja, and H. Rohrer, J. Appl. Phys. **86**, 1898 (1999).